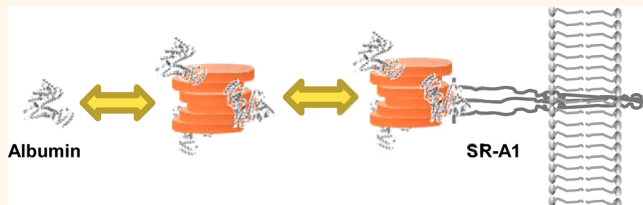


Cryptic Epitopes of Albumin Determine Mononuclear Phagocyte System Clearance of Nanomaterials

Gysell M. Mortimer,[†] Neville J. Butcher,[†] Anthony W. Musumeci,[‡] Zhou J. Deng,[†] Darren J. Martin,[‡] and Rodney F. Minchin^{†,*}

[†]School of Biomedical Sciences and [‡]Australian Institute for Bioengineering and Nanotechnology, University of Queensland, Brisbane, Queensland, 4072, Australia. Experimental work was performed by G.M.M., N.J.B., A.W.M., and Z.J.D. Experimental design and data analysis were performed by G.M.M., D.J.M., and R.F.M. Manuscript was written by all authors.

ABSTRACT While plasma proteins can influence the physicochemical properties of nanoparticles, the adsorption of protein to the surface of nanomaterials can also alter the structure and function of the protein. Here, we show that plasma proteins form a hard corona around synthetic layered silicate nanoparticles (LSN) and that one of the principle proteins is serum albumin. The protein corona was required for recognition of the nanoparticles by scavenger receptors, a major receptor family associated with the mononuclear phagocyte system (MPS). Albumin alone could direct nanoparticle uptake by human macrophages, which involved class A but not class B scavenger receptors. Upon binding to LSN, albumin unfolded to reveal a cryptic epitope that could also be exposed by heat denaturation. This work provides an understanding of how albumin, and possibly other proteins, can promote nanomaterial recognition by the MPS without albumin requiring chemical modification for scavenger receptor recognition. These findings also demonstrate an additional function for albumin *in vivo*.



KEYWORDS: scavenger receptor · protein corona · layered silicate nanoparticles · mononuclear phagocyte system · albumin

Foreign bodies including nanoparticles that enter the circulation interact with the mononuclear phagocyte system (MPS), a global macrophage system in the liver, spleen, and bone marrow.¹ Nanoparticle clearance occurs particularly in the liver and splenic tissue.^{2,3} The MPS is an important determinant of the biological activity for many nanomedicines because they are rapidly cleared by this system *in vivo*. In addition, variation in the function of the MPS has been attributed to clinical variation in the pharmacokinetics and pharmacodynamics of nanoparticle-based drug delivery agents in patients.⁴ Macrophages are phagocytic cells that will engulf particles distinguished by their bearing of recognized opsonins, such as serum proteins that have adsorbed to nanoparticles.^{5,6} For example, polystyrene nanoparticles that adsorb fibronectin, complement protein C3, or immunoglobulin G (IgG) are cleared by hepatic Kupffer cells, specialized phagocytic cells of the liver.^{7,8} Accordingly, some nanoparticles that are accumulated by the MPS show

organ-selective toxicity, especially in the liver.⁹

The principle strategy used to evade the MPS uses polyethylene glycol (PEGylation), a hydrophilic polymer, which is added to the surface of the nanoparticles. This reduces serum protein binding through a process of steric hindrance, thus inhibiting recognition by macrophages.¹⁰ However, this approach is not without issues, as a number of studies have shown increased MPS-dependent clearance of PEGylated nanoparticles following repeated administration.^{11–14} These results emphasize the need to better understand the molecular processes that lead to nanoparticle localization in the MPS. Nanoparticles bind a range of blood proteins that form a surface-associated corona that contributes to the biological identity of circulating nanoparticles.^{15–17} Which of these proteins contribute to the targeting of nanoparticles to the MPS is not well understood. This is highlighted by the fact that protein association with nanoparticles can enhance or reduce localization in the MPS.

* Address correspondence to r.minchin@uq.edu.au.

Received for review November 11, 2013 and accepted March 11, 2014.

Published online March 11, 2014
10.1021/nn405830g

© 2014 American Chemical Society

For example, the use of an albumin coat on particles has shown reduced opsonin receptor-mediated hepatic clearance for some nanoparticles but accumulation in the liver for other nanoparticles.^{18–20}

Natural and synthetic layered silicate nanoparticles (LSNs) are widely used in industries such as food packaging²¹ and cosmetics, and they are under development as drug delivery agents and in polymer nanocomposites with industrial and biomedical applications.^{22,23} We have previously investigated the effect of LSNs on nanocomposites and their potential for enhancing the strength and durability of medically relevant polymers.^{24–26} However, despite growing exposure of humans to these nanoparticles, little is known about their interaction with cells and tissues. Here, we have investigated the interaction of LSNs with a variety of human cells and determined the importance of the protein corona that forms in serum. Albumin was one of the most abundantly adsorbed proteins and could direct macrophage uptake of LSNs. Evidence supporting a role for albumin-directed uptake of nanomaterials by macrophages has been reported for carbonaceous and iron oxide nanoparticles.^{27,28} Structurally damaged albumin is well known to be cleared from the circulation by macrophages.^{29–32} Hence, it is widely assumed that the albumin-directed uptake of foreign particles, including nanomaterials,

by macrophages is due the damaged nature of the associated albumin, especially since albumin acts as a dysopsonin to oppose the effect of opsonins and subsequent MPS clearance.³³ Results from our studies provide a molecular understanding of albumin-directed macrophage uptake by revealing a central role for the unfolding of albumin due to nanoparticle binding and suggest the existence of cryptic epitopes buried within the protein that can act as a ligand for scavenger receptors of the MPS.

RESULTS AND DISCUSSION

LSNs are composed of nanosized platelets with a thickness as small as 1 nm and a diameter ranging from 20 nm to several micrometers depending on their composition, method of synthesis, and purification. This high aspect ratio is, in part, responsible for many of the unique physical and biological properties of these nanoparticles.^{34–36} In solutions, the platelets organize themselves into tactoid structures by face-to-face interactions separated by van der Waals gaps or into microaggregates following edge-to-edge interactions of the individual platelets (Figure 1a).

To study the interaction of LSNs with human cells, we incubated particles labeled with the fluorescent dye YOYO-1 with several cell lines from different tissue origins in complete medium. These included

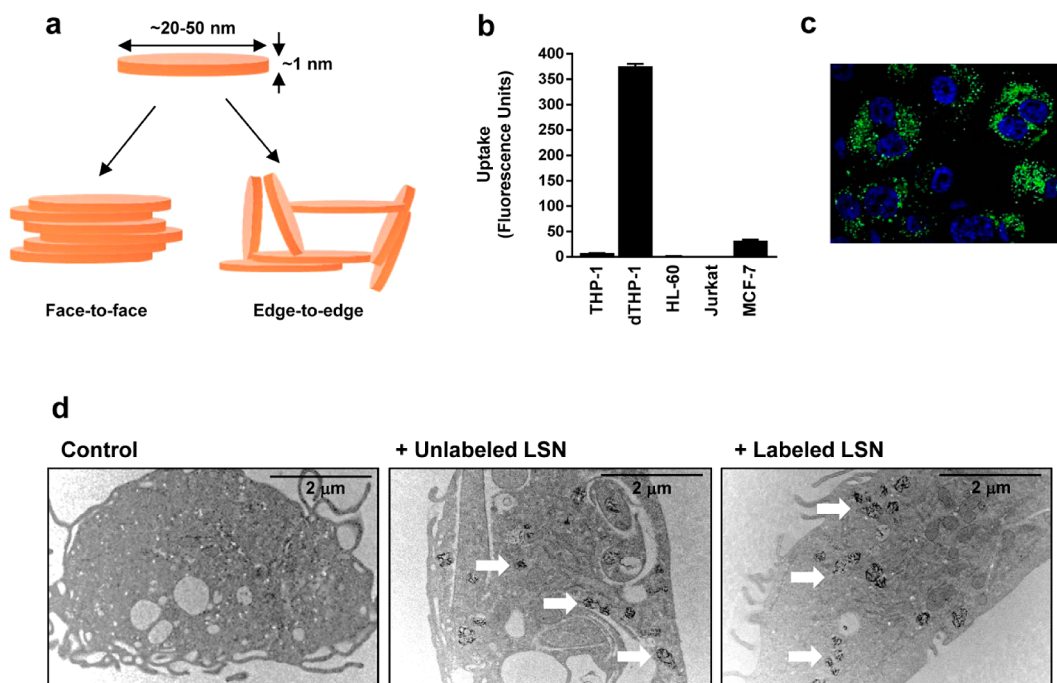


Figure 1. Layered silicate nanoparticle interaction with cells. (a) Representation of the layered silicate nanoparticle (LSN) platelets and their stacking in solution.²³ The present study used layered silicate nanoparticles with an individual disk diameter of 20–50 nm. In solution, these particles agglomerated to structures with a mean hydrodynamic diameter of 85 nm (Supplementary Figure S7). (b) Various human cell lines in complete culture medium were incubated with 10 μ g/mL YOYO-1-labeled nanoparticles for 4 h, and uptake was determined by flow cytometry. Results are mean \pm SEM, $n = 3$. (c) Confocal microscopy of YOYO-1-labeled layered silicate nanoparticles in dTHP-1 cells. Green = nanoparticles, blue = nuclei staining with DAPI. (d) Transmission electron microscopy of dTHP-1 cells in the absence of nanoparticles (left micrograph) or following uptake of unlabeled (center micrograph) or YOYO-1-labeled (right micrograph) nanoparticles. Arrows show electron-dense bodies within intracellular vacuoles. Cells were left unstained in order to better visualize the LSNs.

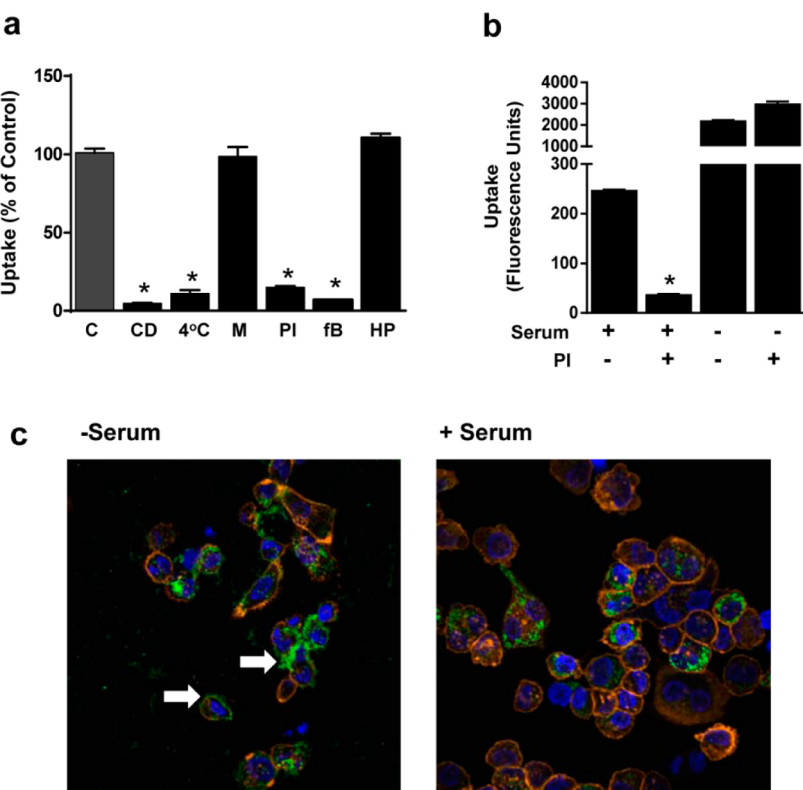


Figure 2. Uptake of layered silicate nanoparticle–protein complexes by dTHP-1 cells. (a) Effect of various endocytosis inhibitors on layered silicate nanoparticle (LSN) uptake by dTHP-1 cells, CD = cytochalasin D (50 μ g/mL); M = mannan (1 mg/mL); PI = polyinosinic acid (100 μ g/mL); fB = formaldehyde-modified bovine albumin (30 μ g/mL); HP = non-heat-inactivated human plasma. Results are mean \pm SEM, $n = 3$. Asterisks indicate significant difference from controls (C). (b) Effect of polyinosinic acid (PI) on the uptake of LSN by dTHP-1 cells in the presence and absence of serum. Results are mean \pm SEM, $n = 3$. Asterisks indicate significant difference from respective controls (−PI). (c) Confocal microscopy of YOYO-1-labeled LSN dTHP-1 cells in the absence and presence of serum. Orange = actin, green = nanoparticles, blue = nuclei staining with DAPI.

the monocytic THP-1 cells, macrophage-like cells obtained by differentiation of THP-1 cells (dTHP-1), the promyelocytic cells HL-60, the T lymphocyte cell line Jurkat, and the epithelial breast cells MCF-7. The average hydrodynamic diameter of LSNs in these experiments was 85 nm. Significant uptake was seen only in the dTHP-1 cells (Figure 1b). This was confirmed by confocal microscopy, which showed punctate cytosolic fluorescence (Figure 1c). Uptake was not due to loss of dye from the nanoparticles, first because of the lack of nuclear fluorescence (YOYO-1 binds with high affinity to DNA) and second because transmission electron microscopy showed localization of the nanoparticles to cellular vacuoles similar to that seen by confocal microscopy. This was true for both YOYO-1-labeled and unlabeled nanoparticles (Figure 1d). Energy-dispersive X-ray spectroscopy was used to verify the electron-dense bodies as LSNs by comparing their magnesium content with surrounding regions of the cell (Supplementary Figure S1).

We next investigated the mechanism of cellular accumulation using several different pharmacological inhibitors of endocytosis and phagocytosis. Differentiated THP-1 cells exhibit many characteristics of human macrophages, which internalize foreign material

by a number of distinct processes.^{3,37} As well as pinocytosis, macrophages specialize in phagocytosis by endocytosis mechanisms involving scavenger receptors, mannose receptors, Fc receptors, and complement receptors. Cytochalasin D inhibits phagocytosis without affecting pinocytosis by specifically disrupting actin formation.³⁸ When dTHP-1 cells were pretreated with cytochalasin D, uptake of LSNs was almost completely suppressed (Figure 2a). A similar result was seen at 4 °C. To interrogate specific endocytosis pathways, cells were treated with the scavenger receptor inhibitor polyinosinic acid and formaldehyde-modified albumin, both of which significantly inhibited uptake. However, the mannose receptor inhibitor mannan had no effect. The possible involvement of complement and Fcγ receptors, which are known to promote uptake of pathogens and apoptotic cells by macrophages,³⁹ could not be assessed using commercial bovine serum because these proteins are removed or inactivated during processing.⁴⁰ Therefore, we used freshly isolated non-heat-inactivated human plasma containing the complete complement and Fc components. We also used serum collected in the absence of anticoagulant additives, many of which reportedly can inhibit complement, with and without complement activation using

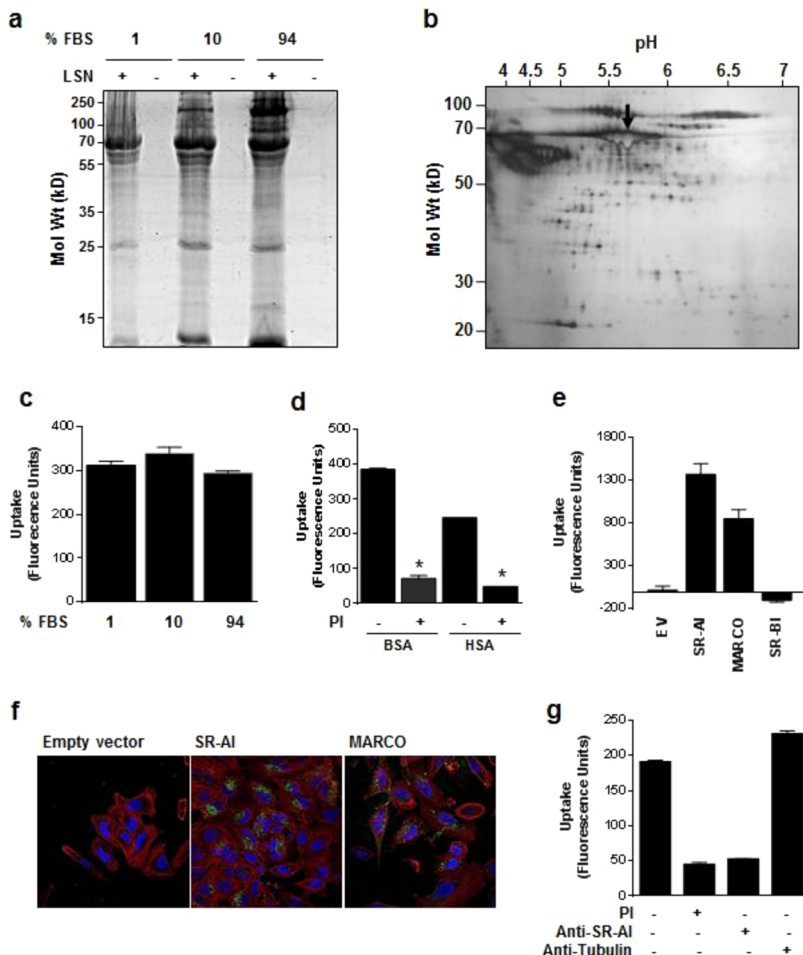


Figure 3. Protein binding to layered silicate nanoparticles. (a) SDS-PAGE of layered silicate nanoparticle (LSN)-bound proteins with increasing bovine serum concentrations. For controls, no nanoparticle was included. (b) Two-dimensional gel electrophoresis of proteins bound to LSN following incubation with bovine serum (1%). Arrow indicates albumin identified by pI and molecular weight. Note the negative staining near the arrow due to excess presence of protein. (c) Uptake of LSNs into dTHP-1 cells in the presence of increasing concentrations of bovine serum. Results are mean \pm SEM, $n = 3$. (d) Uptake of LSNs into dTHP-1 cells in the presence of bovine and human albumin. Cells were also incubated with the scavenger receptor inhibitor polyinosinic acid (PI). Results are mean \pm SEM, $n = 3$. Asterisks indicate significant difference from respective controls (−PI). (e) Uptake of LSNs by scavenger receptor family A members (SR-AI and MARCO) or scavenger receptor family B member (SR-BI) ectopically expressed in HeLa cells. EV = empty vector control. Results are mean \pm SEM, $n = 3$. (f) Confocal microscopy of LSNs in HeLa cells transfected with empty vector, SR-AI, or MARCO. Orange = actin, green = nanoparticles, blue = nuclei staining with DAPI. (g) Uptake of LSNs into dTHP-1 cells in the presence of bovine serum is inhibited by anti-SR-AI antibody but not by an isotype control antitubulin antibody. PI is included as a positive control. Results are mean \pm SEM, $n = 3$.

zymosan. However, we saw no difference in nanoparticle uptake under any of these conditions, indicating that complement and Fc γ receptors are not involved in LSN uptake. These results show that LSNs accumulate in dTHP-1 cells by scavenger receptor-mediated endocytosis.

To determine whether the protein corona was required for uptake, experiments were performed in the presence and absence of serum (Figure 2b). First, cell-associated fluorescence was significantly greater in the absence of serum compared to that in the presence of serum. Confocal microscopy showed that the nanoparticles were mostly associated with the surface of the cells in the absence of serum (Figure 2c, arrows), although a few internalized particles were present

as well. In the presence of serum, surface binding was not evident, suggesting efficient internalization under these conditions. Finally, polyinosinic acid did not inhibit uptake in the absence of serum but, similar to that shown in Figure 2a, almost completely blocked uptake in the presence of serum (Figure 2b). Taken together, these results show that serum is essential for scavenger receptor-mediated uptake of LSNs.

Surface-bound serum proteins were examined by gel electrophoreses. Figure 3a shows the protein binding pattern with increasing bovine serum. There was a major band between 65 and 70 kD that was independent of serum concentration. This band was confirmed as albumin by two-dimensional electrophoresis

based on molecular weight and pI (Figure 3b, arrow). A second major band of approximately 150 kD that increased in intensity with increasing serum was also seen (Figure 3a). However, uptake of LSNs was not affected by an increase in serum concentration (Figure 3c), indicating this larger protein(s) was not involved. This observation is important, as other researchers have reported that different buffer systems can influence the binding affinity of proteins for nanoparticles.⁴¹ The use of high serum concentrations minimizes this possibility.

Albumin binding to other nanomaterials has been extensively reported⁴² and may form part of the tightly bound hard corona or rapidly exchanging soft corona depending on particle surface and size characteristics.^{42,43} However, the molecular mechanisms of this interaction and biological consequences remain largely unknown. Therefore, we next examined the effect of both bovine and human albumin on LSN uptake by dTHP-1 cells (Figure 3d). Both albumins promoted uptake in a polyinosinic acid-dependent manner, suggesting albumin alone can promote the recognition of LSN by scavenger receptors as seen with serum.

Scavenger receptors are composed of a family of proteins that are differentially expressed *in vivo* and exhibit different substrate specificities.⁴⁴ To determine which scavenger receptor might be responsible for nanoparticle uptake, HeLa cells were transfected with constructs expressing SR-AI, MARCO, or SR-BI receptors. Figure 3e shows uptake of LSNs in serum by both SR-AI and MARCO but not by SR-BI. Uptake was confirmed by confocal microscopy (Figure 3f). The lack of uptake by SR-BI was not due to low expression or a lack of function since the SR-BI substrate, oxidized low-density lipoprotein, was taken up into HeLa cells transfected with this receptor (Supplementary Figure S2). In addition, SR-BI expression has been shown in THP-1 cells,⁴⁵ but we did not see uptake in this cell line (Figure 1b), further supporting their lack of a role in LSN uptake. To determine whether uptake of LSNs primarily involved SR-AI in the dTHP-1 cells, we preincubated the cells with anti-human SR-AI antibody to selectively neutralize the uptake pathway (Figure 3g). The antibody inhibited uptake to the same extent as polyinosinic acid, confirming the primary role of this receptor in LSN uptake. Native albumin is not a ligand for scavenger receptors. However, chemically modified albumin (also referred to as structurally "damaged" albumin) is well known to be cleared from the circulation by scavenger receptors.^{29–32} The recognition of modified albumin by specific receptors has been shown to depend on the type of modification.^{46,47}

Therefore, on the basis of our evidence that albumin directs LSN uptake, we reasoned that its interaction with LSNs might lead to conformational changes that

exposed an epitope, or peptide sequence(s), recognized by scavenger receptors. To assess this, we first examined the effect of LSNs on the secondary structure of bovine albumin by far-UV circular dichroism. The nanoparticles alone did not affect ellipticity (Figure 4a, green curve). By contrast, addition of LSN to albumin resulted in a concentration-dependent loss of α -helices, as shown by the increase in ellipticity at 208 and 222 nm (Figure 4a). These observations are consistent with nanoparticle-induced unfolding of the protein.

We next asked whether unfolding albumin by an alternative process could similarly expose an epitope that bound to scavenger receptors. Thermal denaturation of albumin has been extensively studied and has shown that the protein unfolds by at least two processes. The first occurs as the protein is heated to approximately 60 °C and is characterized by refolding upon cooling to 37 °C. The second occurs at temperatures above 60 °C, whereupon the protein does not refold after cooling.⁴⁸ This is demonstrated in Figure 4b using circular dichroism. Bovine albumin was heated to 55 °C and found to refold upon cooling. However, when it was heated to higher temperatures, it did not completely refold. Figure 4c shows that when fluorescently labeled bovine albumin was heat-treated in a similar manner and then incubated with dTHP-1 cells, uptake was seen when refolding did not take place (*i.e.*, heating above 55 °C). This was true for both bovine and human albumin (Figure 4d). Moreover, cell uptake of the heat-denatured proteins is scavenger receptor mediated, as it was almost completely inhibited by polyinosinic acid (Figure 4d). The lack of uptake at 37 °C of non-denatured albumin also indicates that the fluorescent label was not involved in receptor recognition.

Albumin is a globular protein that specifically binds both endogenous and exogenous substrates.⁴⁹ It has three structurally similar domains (Figure 5a) that have been independently expressed and used to map the different binding regions of the protein. To identify the location of any cryptic epitope within the albumin molecule that recognizes the scavenger receptor, we expressed each of the three domains of human albumin (Figure 5a), fluorescently labeled them, and then assessed their uptake by dTHP-1 cells following heat denaturation. The polypeptides of domains I and II interacted with the cells to a greater extent following heating, indicating that they had folded sufficiently after synthesis to hide the peptide region(s) that bind to the scavenger receptor (Supplementary Figure S3). Moreover, polyinosinic acid inhibited the uptake of both of these polypeptides, while it slightly increased that for domain III (Figure 5b). These results suggest scavenger receptor-mediated uptake of domains I and II but not III. Finally, when each of the albumin polypeptides was mixed with the LSNs, 90% or more bound to form peptide–nanoparticle complexes

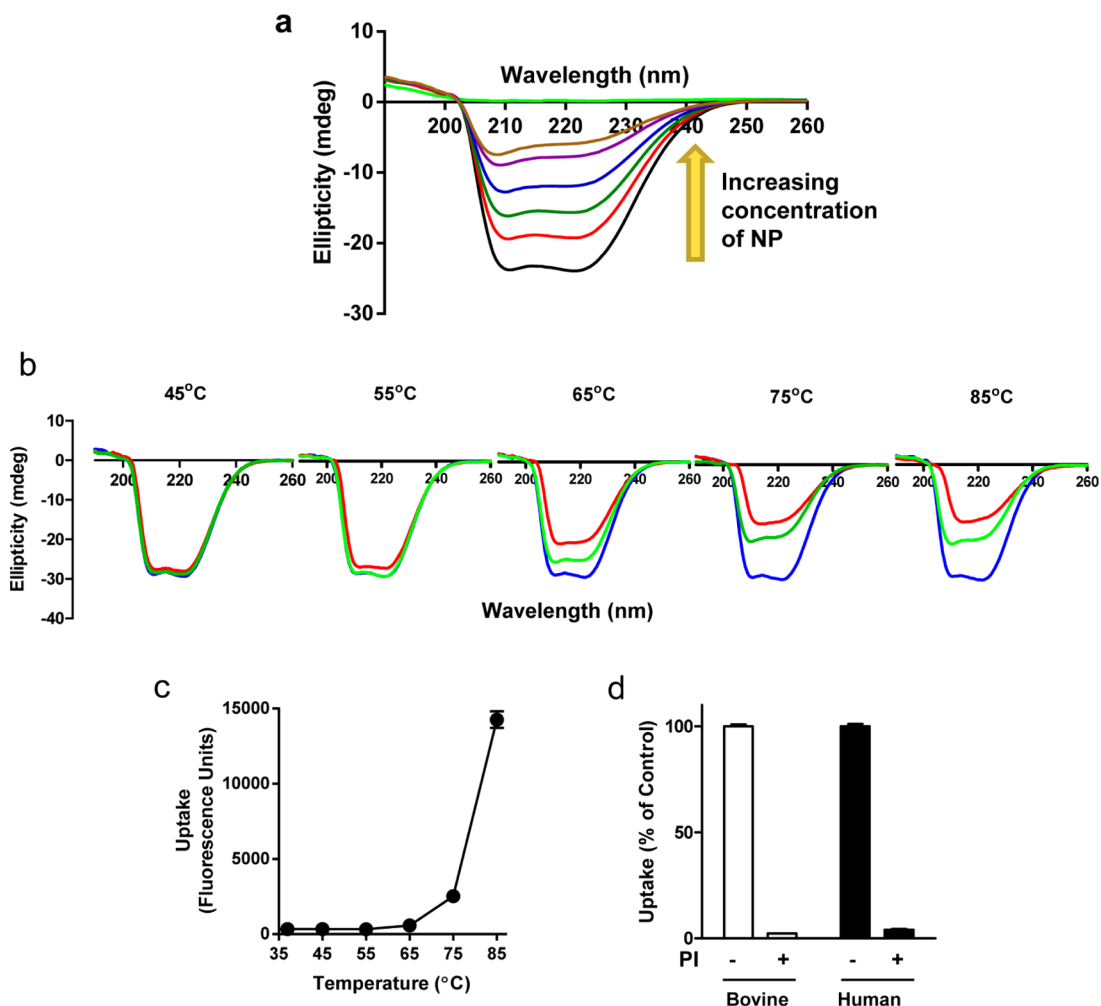


Figure 4. Albumin binding to layered silicate nanoparticles induces protein unfolding. (a) Circular dichroism of bovine albumin (20 µg/mL) with increasing concentrations of nanoparticle (black = 0 µg/mL, red = 2.5 µg/mL, green = 5 µg/mL, blue = 10 µg/mL, violet = 20 µg/mL, brown = 40 µg/mL). (b) Circular dichroism of bovine albumin heated from 37 °C to 45–85 °C followed by cooling to 37 °C. Blue = 37 °C before heating; red = heated temperature; green = 37 °C after heating. (c) Uptake of fluorescently labeled bovine albumin after heating to the indicated temperatures and then cooling to 37 °C. Results are mean \pm SEM, $n = 3$. (d) Effect of polyinosinic acid (PI) on the uptake of heat-denatured (85 °C) bovine and human albumin. Results are mean \pm SEM, $n = 3$.

(Supplementary Figure S4). When dTHP-1 cells were incubated with each of these complexes, uptake of the domain I–LSN complexes and domain II–LSN complexes was inhibited by polyinosinic acid, whereas complexes formed with domain III were not (Figure 5c). These results indicate that denatured polypeptides derived from amino acids 1–186 and 187–380 of human albumin contain sequences that are recognized by scavenger receptors on human dTHP-1 cells.

Our results show that albumin contains cryptic epitopes located in domain I and/or II that promote nanoparticle uptake *via* scavenger receptors. However, as previously mentioned, serum albumin is not normally recognized by this family of receptors, although chemical modification of albumin is well known to promote interaction with both class A and class B receptors.²⁹ These chemical modifications introduce polyanionic regions into the protein, which are

thought to bind to a cluster of positively charged amino acids on the receptor.⁴⁴ Analysis of the human albumin protein sequence identified several polyanionic regions. In domain I, amino acids 56–63 (Asp-Glu-Ser-Ala-Glu-Asp-Cys-Asp) are mostly polyanionic, although these amino acids are located in an exposed loop on the surface of the native protein. In domain II, polyanionic regions are located at amino acids 249–256 (Asp-Leu-Leu-Glu-Cys-Ala-Asp-Asp) and 292–301 (Glu-Val-Glu-Asn-Asp-Glu-Met-Pro-Ala-Asp). Both are buried to varying degrees within the protein. Domain III does not contain any obvious regions of strong negativity. Whether any of these amino acid sequences are responsible for recognition by scavenger receptors following albumin unfolding remains to be determined.

Conformational changes in albumin following binding to different surfaces has been reported, including

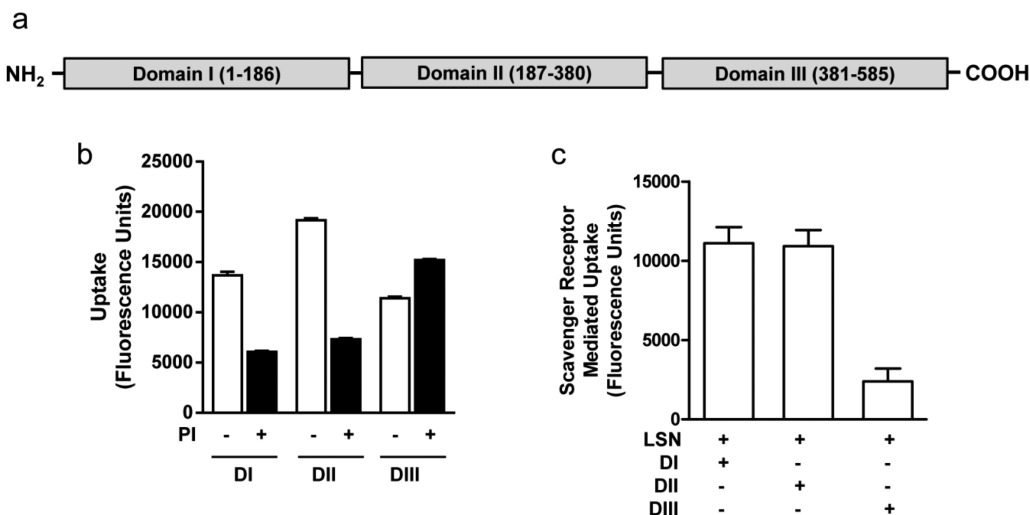


Figure 5. Isolation of the region of albumin responsible for scavenger receptor recognition. (a) Diagrammatic representation of the three domains of human albumin. Amino acid sequence for each is shown in parentheses. (b) Effect of polyinosinic acid (PI) on the uptake of heat-denatured (85 °C) polypeptides (DI = domain I; DII = domain II; DIII = domain III). Results are mean \pm SEM, $n = 3$. (c) Scavenger receptor-mediated uptake of layered silicate nanoparticles complexed with the different albumin domains, determined as the amount of total uptake inhibited by polyinosinic acid. Results are mean \pm SEM, $n = 3$.

soft contact lens material and surface-modified gold particles.^{50–52} Thus, the mechanism described here may have wider applicability across nanotechnology and nanomedicines. However, not all interactions of nanoparticles with albumin result in tight binding and unfolding. Rocker *et al.*⁴³ investigated the binding of albumin to polymer-coated FePt and CdSe/ZnS particles and found low-affinity interactions (micromolar dissociation constants) with relatively rapid exchange rates. Larsericsdotter *et al.* studied the binding of albumin to silica and showed that, while the structural stability of the protein was reduced, there was no evidence that internal residues were exposed to the surrounding environment.⁴¹ Their work indicated loss of tertiary structure without a loss of secondary structure, unlike that reported here (Figure 4a). Other investigators have precoated polystyrene nanoparticles with albumin to prevent opsonization by other serum proteins and reported a decrease in hepatic clearance.¹⁹ On the basis of our evidence that LSN–albumin uptake is structure dependent, we propose that the class of scavenger receptor promoting uptake may change depending on the structural configuration produced as the protein unfolds. For other albumin adsorbing nanomaterials, subsequent unfolding may produce other class-specific recognition structures. This idea is supported by previous studies using colloidal gold. Schnitzer *et al.* reported that the albumin–gold particles bound to two glycoprotein receptors with higher affinity than native albumin.^{53,54} The receptors gp18 and gp30 were originally described as endothelial cell proteins, but have since been found in many tissues and cell types.^{53,55} Importantly, Schnitzer and colleagues reported that the conjugation of albumin to the gold particles induced

conformational changes to the protein that lead to uptake by gp18 and gp30 receptors. These studies, together with our results, suggest that the consequences of albumin binding to nanomaterials will vary considerably depending on the specific characteristics of the protein–nanoparticle interaction and highlight that the presence of a protein in the protein corona is insufficient to predict its influence on the biological identity of the nanoparticle. Since scavenger receptors recognize many modified proteins, it is possible that the unfolding of proteins reveals other scavenger receptor epitopes. Hence, many proteins may serve as opsonins for scavenger receptor clearance as a result of adsorption-induced unfolding. In addition, it is feasible that many other plasma proteins could express similar properties to those we present here for albumin and direct other receptor-specific binding upon unfolding. There is a need to interrogate this possibility using different nanoparticles that bind serum proteins with high affinity.

CONCLUSION

In summary, the present study shows that albumin binds tightly to synthetic layered silicate nanoparticles and rapidly unfolds. It also promotes uptake into cells that express class A scavenger receptors. Since native albumin is not normally a substrate for these receptors, unfolding reveals a cryptic epitope capable of recognition by SR-AI and MARCO. The consequence of this is internalization of the protein–nanoparticle complex in a receptor-mediated manner. This work provides an understanding of how albumin can promote nanomaterial recognition by the MPS without albumin requiring chemical modification for scavenger receptor recognition. Furthermore, these findings present

a unique molecular mechanism for how albumin, and possibly other serum proteins, can promote the

clearance of nanoparticles from the circulation *via* the MPS.

METHODS

Nanoparticle Characterization and Labeling. Synthetic layered silicate nanoparticles (Lucentite-SWN) were purchased from CBC Co. Ltd., Japan (Tokyo, Japan). Nanoparticles were dispersed in ultrapure H₂O at 0.5 mg/mL using vigorous stirring for 30 min, followed by sonication in an ultrasonic bath for 10 min. Particle size distribution and zeta potential were determined by dynamic light scattering and laser doppler electrophoresis using a Nanosizer Nano ZS (Malvern Instruments). The nanoparticles were labeled by ion exchange with YOYO-1 (Molecular Probes) at a concentration of 2 pmol of dye per microgram of nanoparticle for 24 h at 4 °C (Supplementary Figure S5). Under these conditions, no free label was present in solution at the end of the labeling period, as determined following ultracentrifugation. The labeled nanoparticles were stable, with no loss of fluorescence over 4 h in several different media including water, PBS, RPMI, and culture media (Supplementary Figure S6). The labeling of the LSN did not affect the hydrodynamic diameter or the zeta potential (Supplementary Figure S7). In addition, albumin binding to the surface of the particles did not induce agglomeration with the mean nanoparticle diameter not significantly different in the presence or absence of the protein (Supplementary Figure S8). The zeta potential increased slightly.

One-Dimensional Gel Electrophoresis. LSNs (40 µg) were incubated at 37 °C with fetal bovine serum (FBS) at various concentrations (4 mL total volume) for 30 min before centrifugation at 200000g for 1 h at 4 °C. Serum without nanoparticles was used as a control. The nanoparticle–protein pellets were washed and then resuspended in SDS-containing buffer to final concentrations of 1 mg/mL of nanoparticles, with 2% SDS, 5% β-mercaptoethanol, 10% glycerol, and 62.5 mM Tris-HCl. Samples were then heated at 95 °C for 5 min to desorb particle-bound proteins. 1-D gel electrophoresis was used to separate 45 µL of each sample, which were then stained with Sypro Ruby (Bio-Rad) and imaged.

Two-Dimensional Gel Electrophoresis. Human plasma samples were obtained from eight healthy individuals according to institutional bioethics approval. Blood from each donor was collected in sodium citrate and centrifuged for 5 min at 800g to pellet the blood cells. The supernatants were combined and stored in aliquots at -80 °C. On thawing, the plasma was centrifuged for 2 min at 18000g before use. Nanoparticles in phosphate-buffered saline (150 mM sodium chloride and 10 mM phosphate, pH 7.4 PBS) were incubated with 1% bovine serum or human plasma at 37 °C for 4 h before centrifugation at 200000g for 1 h at 4 °C. Plasma without nanoparticles was used as a control. The nanoparticle–protein pellets were washed and then resuspended in SDS-containing buffer to final concentrations of 1 mg/mL of nanoparticles, with 2% SDS, 5% β-mercaptoethanol, 10% glycerol, and 62.5 mM Tris-HCl. Samples were then heated at 95 °C for 5 min to desorb particle-bound proteins.⁵⁶ The prepared samples were then subjected to 2-D gel electrophoresis as described elsewhere⁵⁶ and stained with silver stain solution (2% potassium carbonate, 0.04% sodium hydroxide, 0.007% formaldehyde, and 0.002% sodium thiosulfate).

Circular Dichroism Spectroscopy. Protein samples in PBS (20 µg/mL) were incubated with increasing amounts of nanoparticles for 5 min at ambient temperature and then at 37 °C for 5 min before each measurement. Circular dichroism spectra were recorded using a Jasco J-815 spectrometer (JASCO Inc.) in a 1 cm path length quartz cell from 190 to 260 nm at 37 °C. Data were collected every 0.5 nm with 1 nm bandwidth and averaged over five scans. For heat denaturing experiments, a gradient of 1 °C/min was applied to the sample from 37 °C to the final temperature, which was maintained for 10 min before the temperature was decreased back to 37 °C at 1 °C/min.

Cell Culture. Cell lines were obtained from the American Type Culture Collection (Manassas, VA, USA). Cells were routinely cultured in RPMI 1640 supplemented with 5% FBS and 1% penicillin/streptomycin and maintained at 37 °C in a humidified atmosphere of 5% CO₂ in air. THP-1 cells were differentiated with 100 ng/mL phorbol-12-myristate-13-acetate for 3 days. Cells were treated with labeled nanoparticle (10 µg/mL) for 4 h, trypsinized, and analyzed by flow cytometry using a BD FACSCanto I (Becton Dickinson Biosciences). Uptake was linear for at least 8 h and up to 100 µg/mL nanoparticles. For studies investigating uptake mechanisms, cells were pretreated with either cytochalasin D (Sigma-Aldrich) for 30 min at 50 µg/mL, polyinosinic acid (Sigma-Aldrich) for 1 h at 100 µg/mL, mannan (Sigma-Aldrich) for 1 h at 1 mg/mL, or mouse monoclonal antibody against human scavenger receptor A (R&D Systems, #MAB27081) for 1 h at 3 µg/mL (mouse monoclonal antibody against human α-tubulin (Cell Signaling, #3873) was used as an isotype control). Inhibitors remained in the medium throughout uptake experiments. Serum-free conditions were conducted using RPMI medium only. Human plasma was collected in EDTA and centrifuged at 1000g for 10 min at 4 °C. Plasma was then removed and used immediately or stored at -80 °C until used. Normal human serum was collected into PET plastic venous collection tubes with no additives (Becton Dickinson Biosciences, #362725) and allowed to clot at room temperature for 1 h and then at 4 °C for 2 h. Serum was then collected by centrifugation at 3000g at 4 °C for 17 min and used immediately or stored at -80 °C until used. Complement-activated serum was generated by incubating normal human serum with 20 µg/mL zymosan (Sigma-Aldrich) at 37 °C for 30 min prior to use. For experiments where serum was replaced with albumin (Calbiochem, Fraction V), a final protein concentration of 2.5 mg/mL was used, which is equivalent to the albumin concentration in 5% FBS.

Uptake of heat-denatured bovine albumin was performed by first labeling albumin with Alexa Fluor 647 carboxylic acid succinimidyl ester (Invitrogen) in carbonate buffer (pH 8.6) and then removing unincorporated label by desalting into PBS using PD-10 columns. Labeled albumin was then heat-denatured by heating at 1 °C/min to several maximal temperatures between 37 and 85 °C for 10 min. The temperature was then decreased at 1 °C/min to 37 °C. To assess uptake, dTHP-1 cells were treated with fluorescently labeled heat-denatured albumin (10 µg/mL) for 4 h, trypsinized, and analyzed by flow cytometry.

Oxidized low-density lipoprotein was prepared by oxidizing human low-density lipoprotein with 5 µM CuSO₄ in PBS for 24 h at 37 °C. The reaction was stopped with 50 mM EDTA and 10 mM butylated hydroxytoluene.^{57–59} Formaldehyde-modified bovine serum albumin (BSA) was prepared as described elsewhere.⁶⁰ Both oxidized low-density lipoprotein and formaldehyde-modified BSA were labeled with FITC (Sigma-Aldrich) following the manufacturer's instructions.

Confocal Microscopy. Differentiated THP-1 cells were grown on coverslips at 2 × 10⁵ cells/cm². Following treatment, cells were washed three times with PBS and then fixed in 4% paraformaldehyde. When required, cells were stained with Phalloidin 647 or Phalloidin 555 (Molecular Probes) according to the manufacturer's instructions. Coverslips were washed with PBS and mounted on glass slides using VectorShield mountant containing DAPI (Vector Laboratories). Confocal images were captured using an Olympus BX61 upright confocal microscope.

Transmission Electron Microscopy. Differentiated THP-1 cells were grown as a monolayer. After treatment, the cells were fixed with 2.5% glutaraldehyde and then postfixed with 1% osmium tetroxide. The cells were embedded in LX 112 resin and sectioned, and unstained images were taken using a JEOL 1010 electron microscope. Elemental analysis was conducted on a JEOL 2010 200 keV analytical electron microscope fitted

with an Oxford thin-window energy-dispersive X-ray spectroscopy detector. Sections were carbon coated for 1 h by glow discharge (Cressington 208 carbon coater) prior to elemental map collection.

Scavenger Receptor Expression in HeLa Cells. Human scavenger receptor class A subclass AI in pRc/CMV (Dr. Les Kobzik, Harvard University, USA) was cloned into pcDNA3. Human macrophage receptor with collagenous structure (MARCO) in pcDNA3 was obtained from Prof. Trujvason (Karolina, Sweden). Human scavenger receptor class B subclass BI in pCMV5 (Prof. Van der Westhuzen, University of Kentucky, USA) was cloned into pcDNA3. pcDNA3 empty vector was used as a control. HeLa cells were transfected with plasmids using Lipofectamine2000 (Invitrogen) following the manufacturer's instructions. Transfected cells were treated with nanoparticles 24 h post-transfection for 4 h, trypsinized, and analyzed by flow cytometry.

Expression and Labeling of Albumin Domains. The three domains of human albumin (D1, 1–558 bp; D2, 559–1140 bp; D3, 1141–1758 bp) were amplified by PCR from HepG2 cDNA using specific primers that incorporated NheI and BamHI restriction sites. Digested PCR fragments were cloned into the same sites of the bacterial expression vector pET28a (+) (Novagen). Clones were sequenced, and purified plasmid DNA was electroporated into the bacterial strain BL21-Codon plus(DE3)-RIL (Stratagene) for protein expression. Cultures were induced with 1 mM isopropyl- β -D-thiogalactopyranoside for 4 h at 30 °C for D1 and D2 or 37 °C for D3. D1 and D2 were soluble and were purified using HisPur cobalt resin (Thermo Scientific). Proteins were eluted with 250 mM imidazole and desalting into PBS using PD-10 columns (Millipore). D3 was purified from washed inclusion bodies by solubilization with 4 M guanidine hydrochloride and then desalting into PBS using a PD-10 column. Proteins were labeled with Alexa Fluor 647 carboxylic acid succinimidyl ester (Invitrogen) in carbonate buffer (pH 8.6), and then unincorporated label was removed by desalting into PBS using PD-10 columns.

Statistical Analysis. All experiments were performed at least three times. Data are presented as the mean \pm SEM. Statistical comparisons between different treatments were assessed by two-tailed *t* tests or one-way ANOVA assuming significance at $p < 0.05$.

Conflict of Interest: The authors declare no competing financial interest.

Acknowledgment. This work was supported by funding from the National Health and Medical Research Council of Australia (569694).

Supporting Information Available: A detailed description of methods followed in this work and additional results are available free of charge via the Internet at <http://pubs.acs.org>.

REFERENCES AND NOTES

- Ernsting, M. J.; Murakami, M.; Roy, A.; Li, S. D. Factors Controlling the Pharmacokinetics, Biodistribution and Intratumoral Penetration of Nanoparticles. *J. Controlled Release* **2013**, *172*, 782–794.
- Hume, D. A. The Mononuclear Phagocyte System. *Curr. Opin. Immunol.* **2006**, *18*, 49–53.
- Minchin, R. F.; Martin, D. J. Nanoparticles for Molecular Imaging—An Overview. *Endocrinology* **2010**, *151*, 474–481.
- Caron, W. P.; Song, G.; Kumar, P.; Rawal, S.; Zamboni, W. C. Interpatient Pharmacokinetic and Pharmacodynamic Variability of Carrier-Mediated Anticancer Agents. *Clin. Pharmacol. Ther.* **2012**, *91*, 802–812.
- Moghimi, S. M.; Hunter, A. C. Capture of Stealth Nanoparticles by the Body's Defences. *Crit. Rev. Ther. Drug Carrier Syst.* **2001**, *18*, 527–550.
- Opanasopit, P.; Nishikawa, M.; Hashida, M. Factors Affecting Drug and Gene Delivery: Effects of Interaction with Blood Components. *Crit. Rev. Ther. Drug Carrier Syst.* **2002**, *19*, 191–233.
- Fernandez-Urrusuno, R.; Fattal, E.; Rodrigues, J. M., Jr.; Feger, J.; Bedossa, P.; Couvreur, P. Effect of Polymeric Nanoparticle Administration on the Clearance Activity of the Mononuclear Phagocyte System in Mice. *J. Biomed. Mater. Res.* **1996**, *31*, 401–408.
- Nagayama, S.; Ogawara, K.; Fukuoka, Y.; Higaki, K.; Kimura, T. Time-Dependent Changes in Opsonin Amount Associated on Nanoparticles Alter Their Hepatic Uptake Characteristics. *Int. J. Pharm.* **2007**, *342*, 215–221.
- Nishimori, H.; Kondoh, M.; Isoda, K.; Tsunoda, S.; Tsutsumi, Y.; Yagi, K. Silica Nanoparticles as Hepatotoxicants. *Eur. J. Pharm. Biopharm.* **2009**, *72*, 496–501.
- Jones, S. W.; Roberts, R. A.; Robbins, G. R.; Perry, J. L.; Kai, M. P.; Chen, K.; Bo, T.; Napier, M. E.; Ting, J. P.; Desimone, J. M.; et al. Nanoparticle Clearance is Governed by Th1/Th2 Immunity and Strain Background. *J. Clin. Invest.* **2013**, *123*, 3061–3073.
- Dams, E. T.; Laverman, P.; Oyen, W. J.; Storm, G.; Scherphof, G. L.; van Der Meer, J. W.; Corstens, F. H.; Boerman, O. C. Accelerated Blood Clearance and Altered Biodistribution of Repeated Injections of Sterically Stabilized Liposomes. *J. Pharmacol. Exp. Ther.* **2000**, *292*, 1071–1079.
- Ishida, T.; Ichihara, M.; Wang, X.; Kiwada, H. Spleen Plays an Important Role in the Induction of Accelerated Blood Clearance of Pegylated Liposomes. *J. Controlled Release* **2006**, *115*, 243–250.
- Kaminskas, L. M.; McLeod, V. M.; Porter, C. J.; Boyd, B. J. Differences in Colloidal Structure of Pegylated Nanomaterials Dictate the Likelihood of Accelerated Blood Clearance. *J. Pharm. Sci.* **2011**, *100*, 5069–5077.
- Shiraishi, K.; Hamano, M.; Ma, H.; Kawano, K.; Maitani, Y.; Aoshi, T.; Ishii, K. J.; Yokoyama, M. Hydrophobic Blocks of PEG-Conjugates Play a Significant Role in the Accelerated Blood Clearance (ABC) Phenomenon. *J. Controlled Release* **2013**, *165*, 183–190.
- Walczak, D.; Bombelli, F. B.; Monopoli, M. P.; Lynch, I.; Dawson, K. A. What the Cell "Sees" in Bionanoscience. *J. Am. Chem. Soc.* **2010**, *132*, 5761–5768.
- Monopoli, M. P.; Bombelli, F. B.; Dawson, K. A. Nanobiotechnology: Nanoparticle Coronas Take Shape. *Nat. Nanotechnol.* **2011**, *6*, 11–12.
- Monopoli, M. P.; Aberg, C.; Salvati, A.; Dawson, K. A. Biomolecular Coronas Provide the Biological Identity of Nanosized Materials. *Nat. Nanotechnol.* **2012**, *7*, 779–786.
- Furumoto, K.; Ogawara, K.; Nagayama, S.; Takakura, Y.; Hashida, M.; Higaki, K.; Kimura, T. Important Role of Serum Proteins Associated on the Surface of Particles in Their Hepatic Disposition. *J. Controlled Release* **2002**, *83*, 89–96.
- Ogawara, K.; Furumoto, K.; Nagayama, S.; Minato, K.; Higaki, K.; Kai, T.; Kimura, T. Pre-Coating with Serum Albumin Reduces Receptor-Mediated Hepatic Disposition of Polystyrene Nanosphere: Implications For Rational Design of Nanoparticles. *J. Controlled Release* **2004**, *100*, 451–455.
- Oberdorster, G. Safety Assessment for Nanotechnology and Nanomedicine: Concepts of Nanotoxicology. *J. Intern. Med.* **2010**, *267*, 89–105.
- Chun, A. L. Will the Public Swallow Nanofood? *Nat. Nanotechnol.* **2009**, *4*, 790–791.
- Patel, H. A.; Soman, R. S.; Bajaj, H. C.; Jasra, R. V. Nanoclays for Polymer Nanocomposites, Paints, Inks, Greases and Cosmetics Formulations, Drug Delivery Vehicle and Waste Water Treatment. *Bull. Mater. Sci.* **2006**, *29*, 133–145.
- Pavlidou, S.; Papaspyrides, C. D. A Review on Polymer-Layered Silicate Nanocomposites. *Prog. Polym. Sci.* **2008**, *33*, 1119–1198.
- Osman, A. F.; Edwards, G. A.; Schiller, T. L.; Andriani, Y.; Jack, K. S.; Morrow, I. C.; Halley, P. J.; Martin, D. J. Structure-Property Relationships in Biomedical Thermoplastic Polyurethane Nanocomposites. *Macromolecules* **2012**, *45*, 198–210.
- Andriani, Y.; Jack, K. S.; Gilbert, E. P.; Edwards, G. A.; Schiller, T. L.; Strounina, E.; Osman, A. F.; Martin, D. J. Organization of Mixed Dimethylidioctadecylammonium and Choline Modifiers on the Surface of Synthetic Hectorite. *J. Colloid Interface Sci.* **2013**, *409*, 72–79.

26. Andriani, Y.; Morrow, I. C.; Taran, E.; Edwards, G. A.; Schiller, T. L.; Osman, A. F.; Martin, D. J. *In Vitro* Biostability of Poly(Dimethyl Siloxane/Hexamethylene Oxide)-Based Polyurethane/Layered Silicate Nanocomposites. *Acta Biomater.* **2013**, *9*, 8308–8317.

27. Raynal, I.; Prigent, P.; Peyramaure, S.; Najid, A.; Rebuzzi, C.; Corot, C. Macrophage Endocytosis of Superparamagnetic Iron Oxide Nanoparticles: Mechanisms and Comparison of Ferumoxides and Ferumoxtran-10. *Invest. Radiol.* **2004**, *39*, 56–63.

28. Dutta, D.; Sundaram, S. K.; Teeguarden, J. G.; Riley, B. J.; Fifield, L. S.; Jacobs, J. M.; Addleman, S. R.; Kaysen, G. A.; Moudgil, B. M.; Weber, T. J. Adsorbed Proteins Influence the Biological Activity and Molecular Targeting of Nanomaterials. *Toxicol. Sci.* **2007**, *100*, 303–315.

29. Jansen, R. W.; Molema, G.; Harms, G.; Kruit, J. K.; van Berkel, T. J.; Hardonk, M. J.; Meijer, D. K. Formaldehyde Treated Albumin Contains Monomeric and Polymeric Forms That Are Differently Cleared by Endothelial and Kupffer Cells of the Liver: Evidence for Scavenger Receptor Heterogeneity. *Biochem. Biophys. Res. Commun.* **1991**, *180*, 23–32.

30. Kamps, J. A.; Morselt, H. W.; Swart, P. J.; Meijer, D. K.; Scherphof, G. L. Massive Targeting of Liposomes, Surface-Modified with Anionized Albumins, to Hepatic Endothelial Cells. *Proc. Natl. Acad. Sci. U.S.A.* **1997**, *94*, 11681–11685.

31. Demoy, M.; Andreux, J. P.; Weingarten, C.; Gouritin, B.; Guilloux, V.; Couvreur, P. *In Vitro* Evaluation of Nanoparticles Spleen Capture. *Life Sci.* **1999**, *64*, 1329–1337.

32. Hamblin, M. R.; Miller, J. L.; Ortell, B. Scavenger-Receptor Targeted Photodynamic Therapy. *Photochem. Photobiol.* **2000**, *72*, 533–540.

33. Landsiedel, R.; Fabian, E.; Ma-Hock, L.; van Ravenzwaay, B.; Wohlleben, W.; Wiench, K.; Oesch, F. Toxicity/Biokinetics of Nanomaterials. *Arch. Toxicol.* **2012**, *86*, 1021–1060.

34. Wagner, H. D. Nanocomposites: Paving the Way to Stronger Materials. *Nat. Nanotechnol.* **2007**, *2*, 742–744.

35. Journeay, W. S.; Suri, S. S.; Fenniri, H.; Singh, B. High-Aspect Ratio Nanoparticles in Nanotoxicology. *Integr. Environ. Assess. Manage.* **2008**, *4*, 128–129.

36. Best, J. P.; Yan, Y.; Caruso, F. The Role of Particle Geometry and Mechanics in the Biological Domain. *Adv. Healthcare Mater.* **2012**, *1*, 35–47.

37. Canton, I.; Battaglia, G. Endocytosis at the Nanoscale. *Chem. Soc. Rev.* **2012**, *41*, 2718–2739.

38. Wills, E. J.; Davies, P.; Allison, A. C.; Haswell, A. D. Cytocalasin B Fails to Inhibit Pinocytosis by Macrophages. *Nat. New. Biol.* **1972**, *240*, 58–60.

39. He, J. Q.; Wiesmann, C.; van Lookeren Campagne, M. A Role of Macrophage Complement Receptor Crig in Immune Clearance and Inflammation. *Mol. Immunol.* **2008**, *45*, 4041–4047.

40. Triglia, R. P.; Linscott, W. D. Titers of Nine Complement Components, Conglutinin and C3b-Inactivator in Adult and Fetal Bovine Sera. *Mol. Immunol.* **1980**, *17*, 741–748.

41. Larsericsdotter, H.; Oscarsson, S.; Buijs, J. Structure, Stability, and Orientation of Bsa Adsorbed to Silica. *J. Colloid Interface Sci.* **2005**, *289*, 26–35.

42. Walkey, C. D.; Chan, W. C. Understanding and Controlling the Interaction of Nanomaterials with Proteins in a Physiological Environment. *Chem. Soc. Rev.* **2012**, *41*, 2780–2799.

43. Rocker, C.; Pottl, M.; Zhang, F.; Parak, W. J.; Nienhaus, G. U. A Quantitative Fluorescence Study of Protein Monolayer Formation on Colloidal Nanoparticles. *Nat. Nanotechnol.* **2009**, *4*, 577–580.

44. Martinez, V. G.; Moestrup, S. K.; Holmskov, U.; Mollenhauer, J.; Lozano, F. The Conserved Scavenger Receptor Cysteine-Rich Superfamily in Therapy and Diagnosis. *Pharmacol. Rev.* **2011**, *63*, 967–1000.

45. Matveev, S.; van der Westhuyzen, D. R.; Smart, E. J. Co-expression of Scavenger Receptor-Bl and Caveolin-1 Is Associated With Enhanced Selective Cholestryl Ester Uptake in THP-1 Macrophages. *J. Lipid Res.* **1999**, *40*, 1647–1654.

46. Haberland, M. E.; Fogelman, A. M. Scavenger Receptor-Mediated Recognition of Maleyl Bovine Plasma Albumin and the Demaleylated Protein in Human Monocyte Macrophages. *Proc. Natl. Acad. Sci. U.S.A.* **1985**, *82*, 2693–2697.

47. Lysko, P. G.; Weinstock, J.; Webb, C. L.; Brawner, M. E.; Elshourbagy, N. A. Identification of a Small-Molecule, Nonpeptide Macrophage Scavenger Receptor Antagonist. *J. Pharmacol. Exp. Ther.* **1999**, *289*, 1277–1285.

48. Flora, K.; Brennan, J. D.; Baker, G. A.; Doody, M. A.; Bright, F. V. Unfolding of Acrylodan-Labeled Human Serum Albumin Probed by Steady-State and Time-Resolved Fluorescence Methods. *Biophys. J.* **1998**, *75*, 1084–1096.

49. Dockal, M.; Carter, D. C.; Ruker, F. Conformational Transitions of the Three Recombinant Domains of Human Serum Albumin Depending on pH. *J. Biol. Chem.* **2000**, *275*, 3042–3050.

50. Castillo, E. J.; Koenig, J. L.; Anderson, J. M.; Lo, J. Characterization of Protein Adsorption on Soft Contact Lenses. I. Conformational Changes of Adsorbed Human Serum Albumin. *Biomaterials* **1984**, *5*, 319–325.

51. Sivaraman, B.; Fears, K. P.; Latour, R. A. Investigation of the Effects of Surface Chemistry and Solution Concentration on the Conformation of Adsorbed Proteins Using an Improved Circular Dichroism Method. *Langmuir* **2009**, *25*, 3050–3056.

52. Smith, J. R.; Cicerone, M. T.; Meuse, C. W. Tertiary Structure Changes in Albumin upon Surface Adsorption Observed via Fourier Transform Infrared Spectroscopy. *Langmuir* **2009**, *25*, 4571–4578.

53. Schnitzer, J. E.; Sung, A.; Horvat, R.; Bravo, J. Preferential Interaction of Albumin-Binding Proteins, Gp30 and Gp18, with Conformationally Modified Albumins. Presence in Many Cells and Tissues with a Possible Role in Catabolism. *J. Biol. Chem.* **1992**, *267*, 24544–24553.

54. Schnitzer, J. E.; Bravo, J. High Affinity Binding, Endocytosis, and Degradation of Conformationally Modified Albumins. Potential Role of Gp30 and Gp18 as Novel Scavenger Receptors. *J. Biol. Chem.* **1993**, *268*, 7562–7570.

55. Ghinea, N.; Fixman, A.; Alexandru, D.; Popov, D.; Hasu, M.; Ghitescu, L.; Eskenasy, M.; Simionescu, M.; Simionescu, N. Identification of Albumin-Binding Proteins in Capillary Endothelial Cells. *J. Cell Biol.* **1988**, *107*, 231–239.

56. Deng, Z. J.; Liang, M.; Monteiro, M.; Toth, I.; Minchin, R. F. Nanoparticle-Induced Unfolding of Fibrinogen Promotes Mac-1 Receptor Activation and Inflammation. *Nat. Nanotechnol.* **2011**, *6*, 39–44.

57. Dejager, S.; Mietus-Synder, M.; Pitas, R. E. Oxidized Low Density Lipoproteins Bind to the Scavenger Receptor Expressed by Rabbit Smooth Muscle Cells and Macrophages. *Arterioscler. Thromb.* **1993**, *13*, 371–378.

58. Beppu, M.; Hora, M.; Kikugawa, K. A Simple Method for the Assessment of Macrophage Scavenger Receptor-Ligand Interaction: Adherence of Erythrocytes Coated with Oxidized Low Density Lipoprotein and Modified Albumin to Macrophages. *Biol. Pharm. Bull.* **1994**, *17*, 39–46.

59. Rhaihards, D.; Falstrault, L.; Tremblay, C.; Brissette, L. Uptake and Fate of Class B Scavenger Receptor Ligands in HepG2 Cells. *Eur. J. Biochem.* **1999**, *261*, 227–235.

60. Horiuchi, S.; Takata, K.; Morino, Y. Characterization of a Membrane-Associated Receptor from Rat Sinusoidal Liver Cells that Binds Formaldehyde-Treated Serum Albumin. *J. Biol. Chem.* **1985**, *260*, 475–481.